Modulation of prostate cancer genetic risk by omega-3 and omega-6 fatty acids

Isabelle M. Berquin,[1,2] Younong Min,[1] Ruping Wu,[1] Jiansheng Wu,[1] Donna Perry,[2] J. Mark Cline,[2] Mike J. Thomas,[3] Todd Thornburg,[4] George Kulik,[1] Adrienne Smith,[1] Iris J. Edwards,[2] Ralph D'Agostino Jr.,[5] Hao Zhang,[6] Hong Wu,[7] Jing X. Kang,[8] and Yong Q. Chen[1,4]

[1]Department of Cancer Biology, [2]Department of Pathology, [3]Department of Biochemistry, [4]Comprehensive Cancer Center, and [5]Department of Biostatistical Science, Wake Forest University School of Medicine, Winston-Salem, North Carolina, USA. [6]Laboratory of Food Biotechnology, School of Food Science and Technology, Southern Yangtze University, Wuxi, People's Republic of China. [7]Department of Molecular and Medical Pharmacology, UCLA David Geffen School of Medicine, Los Angeles, California, USA. [8]Department of Medicine, Massachusetts General Hospital and Harvard Medical School, Boston, Massachusetts, USA.

Although a causal role of genetic alterations in human cancer is well established, it is still unclear whether dietary fat can modulate cancer risk in a predisposed population. Epidemiological studies suggest that diets rich in omega-3 polyunsaturated fatty acids reduce cancer incidence. To determine the influence of fatty acids on prostate cancer risk in animals with a defined genetic lesion, we used prostate-specific *Pten*-knockout mice, an immune-competent, orthotopic prostate cancer model, and diets with defined polyunsaturated fatty acid levels. We found that omega-3 fatty acids reduced prostate tumor growth, slowed histopathological progression, and increased survival, whereas omega-6 fatty acids had opposite effects. Introducing an omega-3 desaturase, which converts omega-6 to omega-3 fatty acids, into the *Pten*-knockout mice reduced tumor growth similarly to the omega-3 diet. Tumors from mice on the omega-3 diet had lower proportions of phosphorylated Bad and higher apoptotic indexes compared with those from mice on omega-6 diet. Knockdown of Bad eliminated omega-3–induced cell death, and introduction of exogenous Bad restored the sensitivity to omega-3 fatty acids. Our data suggest that modulation of prostate cancer development by polyunsaturated fatty acids is mediated in part through Bad-dependent apoptosis. This study highlights the importance of gene-diet interactions in prostate cancer.

Introduction

A causal role of genetic alterations in human cancer is well established; however, environmental influence on cancer risk is not clearly understood. Over 2 decades, epidemiologic studies have been reported on the effect of dietary fat on prostate cancer risk (1). However, the mechanistic role of dietary fat in prostate cancer remains ill defined. Prostate cancer is the most frequently diagnosed cancer and a leading cause of cancer death in men in the US. There is a wide variation in international prostate cancer mortality rates; these are particularly high in Northern Europe and North America and much lower in Japan and other Asian countries (2). Yet small, latent carcinomas of the prostate diagnosed at autopsy are as common in Asian countries as in Western countries (3). Immigrants from Poland and Japan exhibit a significant increase in the risk of developing clinical prostate cancer when resident in the US (4–6). These findings implicate environmental variables, and possibly diet, as significant contributing factors.

Omega-3 and omega-6 polyunsaturated FAs (PUFAs) are essential FAs: mammals can neither synthesize them de novo nor interconvert them; therefore, they have to be taken in from diet. Many vegetable oils contain high levels of omega-6 PUFAs, whereas fish oil is a rich source of omega-3 PUFAs, mainly eicosapentaenoic acid (EPA; 20:5n-3) and docosahexaenoic acid (DHA; 22:6n-3). Diets with an omega-6/omega-3 PUFA ratio of 1 are recommended for human consumption by a panel of nutritionists (7), and diets with a similar ratio are consumed by some populations such as the Inuit (8). Current Western diets have omega-6/omega-3 ratios of approximately 30 (9), although they can be as high as 50 (10) (Supplemental Figure 1; supplemental material available online with this article; doi:10.1172/JCI31494DS1). Some evidence suggests that cyclooxygenase inhibitors, which block the metabolism of omega-6 PUFAs, are beneficial in prevention of colon (11) and prostate (12) cancer. However, the cardiovascular toxicity (13) of cyclooxygenase-2 inhibitors has jeopardized the clinical utility of these drugs. Reducing the intake of omega-6 PUFAs and increasing the proportion of dietary omega-3 is an attractive approach.

Inaccuracy in reporting dietary intake and difficulties in conducting mechanistic studies on human populations have hampered investigations on the role of dietary fat in prostate cancer development. Most experiments using animals have been performed in xenograft models and are limited by the fact that tumors grow at an ectopic site in an immune-deficient host environment. Moreover, dietary composition in animal diets is often poorly defined, and dietary intake is inadequately monitored. In an effort to overcome these limitations, we used prostate-specific *Pten*-knockout mice, an immune-competent, orthotopic prostate cancer model, and designed diets to investigate the influence of dietary PUFAs on prostate cancer risk in animals with this defined genetic lesion.
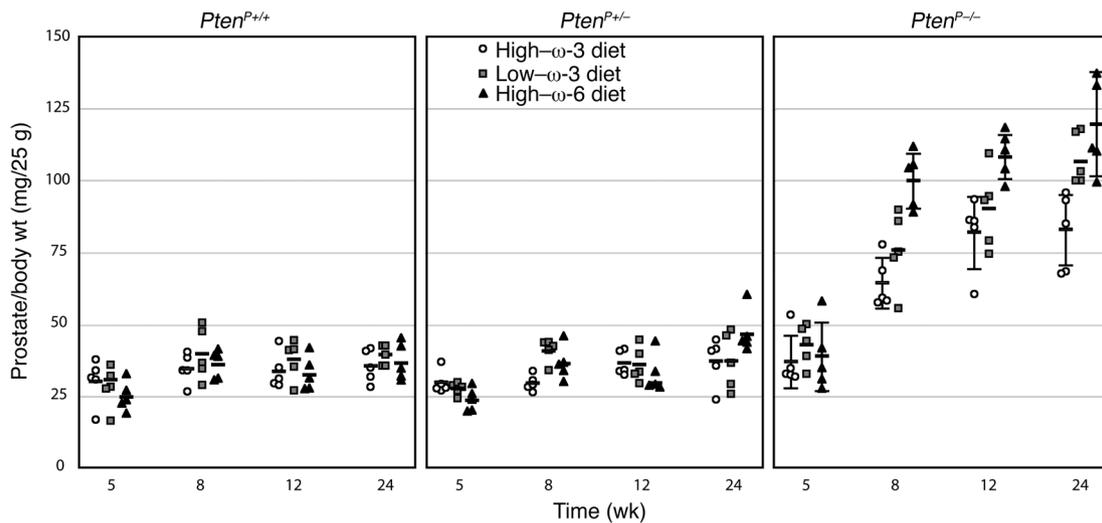
Results

Omega-3 and -6 PUFAs differentially modulate prostate tumor weight in Pten[P–/–] mice. Mice with a defined genetic lesion, in this case loss of the tumor suppressor gene *Pten*, develop cancer spontaneously. To determine whether genetic cancer risk can be modified by dietary

Figure 1
Suppression of prostate tumor proliferation by omega-3 PUFAs in vivo. $Pten^{P+/+}$, $Pten^{P+/-}$, and $Pten^{P-/-}$ mice were fed the high–omega-3, low–omega-3, and high–omega-6 diet for a period of up to 24 weeks. Mouse AP, DL, and VP lobes were weighed, and the sums were expressed as milligrams per 25 gram body weight. Five mice were used per data point in a cohort of 180 mice. Open circles represent mice on the high–omega-3 diet; shaded squares, mice on the low–omega-3 diet; filled triangles, mice on the high–omega-6 diet. Horizontal bars represent averages. SDs are shown for $Pten^{P-/-}$ mice fed with the high–omega-3 and high–omega-6 diet.

factors, wild-type mice and mice with *Pten* deletion were fed diets with different amounts of omega-3 and omega-6 fatty acids. Prostate-specific deletion of floxed *Pten* was achieved by expressing Cre recombinase under the control of a probasin promoter (PB). Mouse genotypes are $Pten^{loxP/loxP}PB$-$cre4^{-/-}$ (wild-type), $Pten^{loxP/+}PB$-$cre4^{T/-}$ (heterozygous), and $Pten^{loxP/loxP}PB$-$cre4^{T/-}$ (homozygous). For simplicity, we hereafter refer to these mice as $Pten^{P+/+}$, $Pten^{P+/-}$, and $Pten^{P-/-}$, respectively. Experimental diets included high–omega-3, low–omega-3, and high–omega-6 diets, with ratios of omega-6/omega-3 PUFAs of 1, 20, and 40, respectively. Diets were designed to be nutritionally balanced, with the same caloric input and percentage of energy from fat (Supplemental Table 1). Omega-6/omega-3 FA ratios in mouse blood and prostate tissues were similar to those in the respective diet (Supplemental Figure 2). In addition, phospholipid profiling demonstrated that approximately 5-fold more omega-3 PUFAs were incorporated at the *sn-2* position in mice fed the high–omega-3 diet compared with mice fed with the low–omega-3 or the–high omega-6 diet (Supplemental Figure 2C). The 3 diets were absorbed equally well in mice of different genotypes at various ages and did not affect body weight (Supplemental Figure 3).

Mice were sacrificed at 5, 8, 12, and 24 weeks of age. After recording mouse body weight, we dissected, photographed, and weighed the anterior, dorsolateral, and ventral prostate (AP, DL, and VP) lobes. In the $Pten^{P+/+}$ and $Pten^{P+/-}$ groups, the relative prostate weight (expressed as mg/25 g body weight) increased from approximately 29 to approximately 35 between 5 and 8 weeks and remained constant thereafter (Figure 1). Diets did not affect the weight or gross appearance of these wild-type prostates. By contrast, the average prostate weight of $Pten^{P-/-}$ mice was significantly higher than that of $Pten^{P+/+}$ or $Pten^{P+/-}$ mice starting at 8 weeks of age (Figure 1). Remarkably, the prostate weight gain from 5 to 24 weeks was significantly less in mice fed the high–omega-3 diet compared with mice fed the high–omega-6 diet, with intermediary gains for mice on the

low–omega-3 diet (Figure 1). Age, treatment, and age/treatment interactions were all statistically significant (treatment, $P < 0.001$; age, $P < 0.001$; interaction, $P = 0.018$).

Omega-3 and -6 PUFAs differentially affect prostate tumor progression to carcinoma in $Pten^{P-/-}$ mice. Prostate lobes from $Pten^{P+/+}$ and $Pten^{P+/-}$ mice appeared morphologically normal at 5–24 weeks of age, regardless of diet. However, prostate lobes from $Pten^{P-/-}$ mice were clearly enlarged and showed increased vascularity as well as cellularity (Figure 2A). Pathological evaluation was performed to determine the presence of hyperplasia, carcinoma in situ (CIS), and invasive carcinoma in AP, DL, and VP lobes of $Pten^{P-/-}$ mice (Figure 2, B and C, and Supplemental Figure 4). DL lobes developed a greater proportion of advanced lesions as compared with AP and VP lobes. Prostates from 8-week-old mice on the high–omega-3 diet were more likely to have normal or benign histology. For instance, all VP lobes from 8-week-old mice on the high–omega-3 diet were either normal or hyperplastic, whereas VP lobes from mice on the high–omega-6 diet frequently contained CIS and invasive carcinoma. Even in the DL lobe, where *Pten* deletion occurs earliest, only half of the mice fed the high–omega-3 diet developed invasive carcinoma, whereas 80% of mice fed the high–omega-6 diet had invasive carcinoma. Mice fed the low–omega-3 diet generally developed prostate lesions with intermediate histopathology.

It is noteworthy that omega-3 PUFAs slowed the histological progression of prostate tumors in 5- to 8-week-old $Pten^{P-/-}$ mice. Once carcinoma developed, omega-3 PUFAs induced apoptosis and decreased the growth of tumor mass. The probasin promoter, which drives the prostate-specific expression of cre, is activated by androgens. Levels of sex hormones increase in male mice around 6 weeks of age, resulting in efficient *Pten* deletion. Activity of the probasin promoter is highest in the lateral prostate followed by anterior and ventral lobes. Accordingly, invasive carcinoma developed earlier in the DL than the VP and AP lobes. To determine whether diets affected the *Pten* deletion rate, which may account
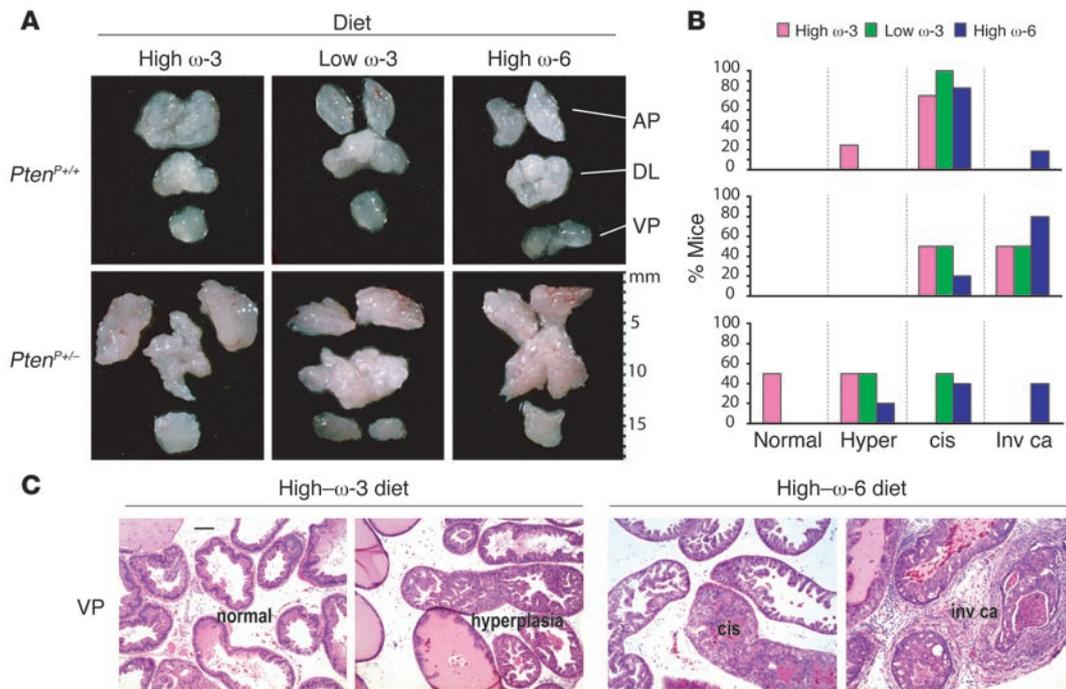
Figure 2
Pathological evaluation of prostate. (**A**) Gross appearance of 8-week-old prostates. (**B**) Histological evaluation of AP, DL, and VP lobes. Histology was evaluated for the cohort of 180 mice used in Figure 1, but qualitative differences were observed for 8-week-old $Pten^{P-/-}$ mice when the high–omega-3, low–omega-3, and high–omega-6 diets were compared. Two sections of AP, DL, and VP from each mouse (5 mice per group) were sampled from separate areas of each tissue block and evaluated by 2 veterinary pathologists. When complex histology was found, the most advanced type was indicated. Hyper, hyperplasia; cis, carcinoma in situ; Inv ca, invasive carcinoma. (**C**) Representative H&E-stained sections from VPs of $Pten^{P-/-}$ mice. Scale bar: 100 μm. Additional sections are shown in Supplemental Figure 3.

for the difference in prostate cancer progression, we used 3 different approaches: (a) real-time quantification of the inactive *Pten* allele (Figure 3, A and B); (b) enzymatic assay of a *lacZ* gene whose expression depends upon Cre activity (Figure 3C); and (c) Western blotting of the active form of Akt, which is indicative of *Pten* inactivation (Figure 3C). Our data showed a similar *Pten* deletion rate in mice on the high–omega-3 diet and the high–omega-6 diet, indicating that this was not a factor in the rate of cancer development.

Genetic validation of the effects of PUFAs on prostate tumor growth. Although dietary ingredients were carefully formulated, the diets necessarily included other fats besides the omega-3 and -6 PUFAs to keep the energy from fat constant (Supplemental Table 1). To eliminate these possible confounding effects, the *fat1* transgene (14), encoding an omega-3 desaturase from *Caenorhabditis elegans* that converts omega-6 into omega-3 FAs, was bred into the prostate-specific *Pten*-knockout genetic background. $Pten^{P-/-}$ mice with or without the *fat1* transgene (*fat1*$^{T/-}$ and *fat1*$^{-/-}$, respectively) were both fed the high–omega-6 diet. Mice were sacrificed at 12 weeks of age, and prostates were dissected and weighed. The average omega-6/omega-3 ratio in the blood and prostate tissues of *fat1*$^{T/-}$ mice was 5, compared with 40 in *fat1*$^{-/-}$ mice (Table 1). Thus, fat-1 was able to convert most of the omega-6 PUFAs to omega-3. Relative prostate weights were significantly lower in $Pten^{P-/-}$*fat1*$^{T/-}$ than that in $Pten^{P-/-}$*fat1*$^{-/-}$ mice (Figure 4; $P < 0.006$, Student's *t* test). This genetic approach confirms the suppressive effect of omega-3 PUFAs on tumor growth observed with diet manipulation. Thus, the *fat1* mouse results are consistent with our conclusion that omega-3 and omega-6 FAs have opposite effects on tumor growth.

Omega-3 and -6 PUFAs differentially affect survival of $Pten^{P-/-}$ mice. Overall survival was also monitored for mice on the 3 different diets. $Pten^{P+/+}$ mice remained free of tumors and had a survival rate of 100% within the time period monitored, regardless of diet. $Pten^{P+/-}$ mice also had a survival rate of 100%, although some prostates from mice on the high–omega-6 diet were hyperplastic or neoplastic. By contrast, the 12-month survival rate for $Pten^{P-/-}$ mice was 60% on the high–omega-3 diet, 10% on the low–omega-3 diet, and 0% on the high–omega-6 diet (Figure 5). In fact, no $Pten^{P-/-}$ mice on the high omega-6 diet survived beyond 10 months of age in our experimental group. The main cause of death was bladder obstruction due to the prostate tumor compressing the urethra. Bladders were visibly dilated in some mice, and a few were even ruptured. These severe cases led to early death. For $Pten^{P-/-}$ mice that survived 6 months or longer, retention of urine in the AP lobes was consistently seen and often accompanied by pyelonephritis. Cox proportional hazards model analysis revealed that diets exerted statistically significant effects on survival ($P = 0.005$). Compared with the high–omega-6 diet, the high–omega-3 diet significantly increased the survival of $Pten^{P-/-}$ mice (hazard ratio 0.137; $P = 0.0016$), and, although to a lesser degree, the low–omega-3 diet significantly increased the survival as well (hazard ratio 0.337; $P = 0.0338$).

Effect of omega-3 and -6 PUFAs on the proapoptotic protein Bad. Pten encodes a phosphatidylinositol phosphatase that negatively regulates the PI3K/Akt signaling pathway. Akt promotes cell survival, protein synthesis, and proliferation when it is activated after being recruited to the plasma membrane by PI(3,4,5)P$_3$ (phosphatidylino-
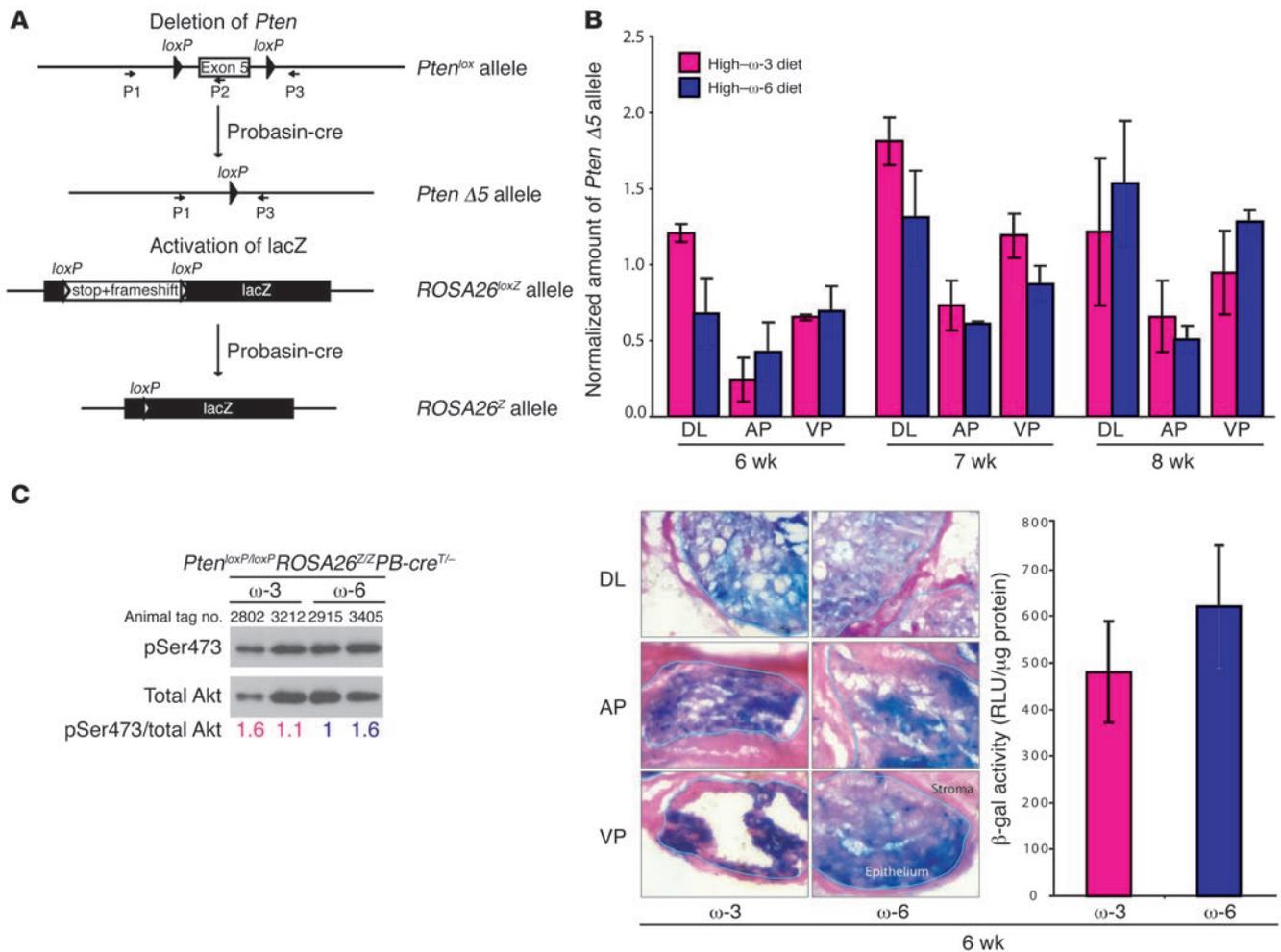
Figure 3
Pten deletion rate in mice on high–omega-3 and high–omega-6 diets. (**A**) Schematic representation of *Pten* and *lacZ* alleles before and after Cre-*loxP*–mediated recombination. In the *ROSA26^LoxZ* allele, recombination removes a sequence that interrupts the coding frame of β-galactosidase, resulting in activation of β-galactosidase enzyme. (**B**) Real-time quantification of *Pten Δ5* allele. The inactive (exon 5 deletion) *Pten* allele and a control gene (wild-type *Il-2*) were quantified in 6-, 7-, and 8-week-old AP, DL, and VP lobes from mice on the high–omega-3 and high–omega-6 diet. Levels of the *Pten Δ5* allele normalized to *Il-2* are shown. Three mice were used for each data point, with bars representing SEM. *Pten* was deleted to similar extents in mice on either diet. (**C**) Prostates from 6-week-old *Pten^loxP/loxP^ROSA26^Z/Z^PB-cre4^T/–* mice on the high–omega-3 and high–omega-6 diet were dissected, snap-frozen, and used for β-galactosidase staining as well as activity measurement. Three mice were used for each data point. Bars represent SEM. Pictures were taken at ×20 magnification. In 4 of the 6 mice that had sufficient protein remaining, the ratio of phosphorylated to total Akt, which is indicative of *Pten* inactivation, was quantified by Western blotting.

sitol [3,4,5] triphosphate). Pten converts PI(3,4,5)P$_3$ to PI(4,5)P$_2$, resulting in lower activity of Akt. Loss of *Pten* is expected to increase Akt activity; therefore, we examined the status of Akt and its downstream signaling effectors in prostate samples of wild-type and *Pten*-knockout mice on the high–omega-3 and high–omega-6 diets.

Pten status or diet had little effect on total Akt protein levels, as measured by Western blotting (Figure 6A). The ratio of active (pSer473) Akt to total Akt protein was approximately 3- to 7-fold higher in prostates from the *Pten^P–/–* mice than those from the *Pten^P+/+* mice. However, there was no significant difference in the active/total Akt ratio between *Pten^P–/–* prostates from mice on the high–omega-3 and high–omega-6 diet (Figure 6A). Among the Akt effectors, the proapoptotic protein Bad was detected at higher levels in *Pten^P–/–* than in *Pten^P+/+* prostates from mice on the high–omega-3 diet but not on the high–omega-6 diet. Additionally, the ratio of phosphorylated

(pSer112) to total Bad was significantly lower in *Pten^P–/–* prostates from mice on the omega-3 diet compared to the omega-6 diet (Figure 6A). Phosphorylation of Bad inhibits its proapoptotic function. Therefore, in mice on the omega-3 diet, the elevated Bad levels combined with a lower fraction of phosphorylated Bad would favor apoptosis. Indeed, a higher number of apoptotic cells was seen in *Pten^P–/–* prostates from mice on the high–omega-3 than on the high–omega-6 diet as determined by immunohistochemistry of cleaved caspase-3 (Figure 6B and Table 2). Other Akt substrates, namely Foxo1 and Foxo3a and p70S6K (product of the gene *Rps6kb1*), were phosphorylated to similar degrees in *Pten^P–/–* prostates regardless of diet (Supplemental Figure 5).

Omega-3, but not omega-6, PUFA induces prostate cancer cell apoptosis in a Bad-dependent manner. Omega-3 PUFA treatment inhibits tumor cell proliferation and induces apoptosis in culture (15).
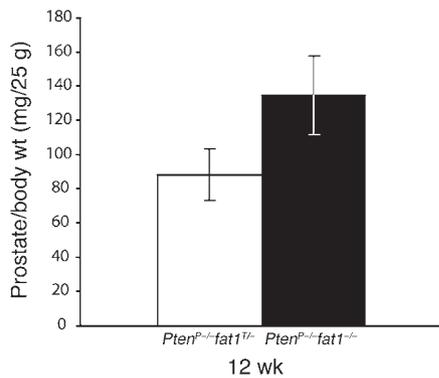
Figure 4
Effect of the fat-1 omega-3 desaturase on prostate tumor growth. $Pten^{P-/-}fat1^{T/-}$ and $Pten^{P-/-}fat1^{-/-}$ mice were fed the high–omega-6 diet. Prostate tumor weight was compared in 12-week-old mice, with 5 mice per group. Bars represent SD. $P < 0.006$, Student's t test.

Since in vivo data suggest that omega-3 PUFAs may induce apoptosis through regulation of Bad, we further investigated the role of Bad in omega-3 PUFA–induced cell death. PC3 and LNCaP cells were mock infected or infected with lentiviruses expressing scrambled or Bad-specific short hairpin RNA (shRNA) (Figure 7A). Successful knockdown of Bad was confirmed by Western blotting (Figure 7A). These cells were then incubated with omega-3 or -6 PUFAs for 6 days, and the total cell number as well as the number of dead cells were determined by trypan blue exclusion. As shown in Figure 7B, in mock- or scrambled shRNA–infected cells, omega-3 PUFA treatment increased the percentage of dead cells, whereas omega-6 PUFA treatment had no significant effect. Strikingly, knockdown of Bad completely eliminated omega-3 PUFA–induced cell death, and the percentage of dead cells was similar to that in untreated cells. By contrast, knockdown of Bad had little effect on omega-6 PUFA–treated cells. To confirm the specificity of the Bad knockdown construct, we introduced mouse Bad cDNA, which cannot be silenced by our shRNA designed to target human Bad. Introduction of Bad cDNA restored prostate cancer cell sensitivity to omega-3–induced cell death but did not significantly increase cell death upon omega-6 treatment (Figure 7C). These results suggest that cell death induced by omega-3 PUFAs is dependent on Bad expression.

Discussion

Although a causal role of genetic alterations in human cancer is well established, epigenetic effects on cancer were not appreciated until recently (16). On the one hand, methylation, acetylation, and other molecular mechanisms implicated in epigenetics are being studied intensively (17, 18), but environmental factors causing these changes are largely unknown. On the other hand, factors such as diet are believed to affect cancer incidence, but molecular mechanisms have not been delineated. Here, we demonstrated the influence of defined dietary factors (omega-3 and -6 essential FAs) on a mouse model of prostate cancer with a known genetic risk (*Pten* deletion) and investigated underlying molecular mechanisms.

Epidemiological studies suggest that consumption of fish or fish oil reduces prostate cancer incidence (19, 20). One of the largest prospective studies, involving 6,272 men with 30 years of follow-up, indicated that fatty fish consumption was associated with decreased risk of prostate cancer (20). Serum levels of omega-3 PUFAs were reported to be significantly lower in patients with benign prostate hyperplasia and prostate cancer, and omega-6 PUFA levels were higher in patients with prostate cancer compared with age-matched controls (21). In prostate tissues, the percentage of total PUFAs was shown to be significantly lower in the presence of perineural invasion, seminal vesicle involvement, and stage T3 tumor. Levels of α linolenic acid (αLNA) omega-3 PUFAs were significantly lower when tumor extended to an anatomical or surgical margin. Total omega-3 levels and omega-3/omega-6 PUFA ratios were 1.5- to 3.3-fold lower in cases than in controls (22). In a 12-year prospective study of 47,882 men participating in the Health Professionals Follow-up Study, higher consumption of fish was strongly associated with a reduced risk of metastatic prostate cancer (23).

Nevertheless, molecular mechanisms of omega-3 PUFA effects on prostate cancer remain elusive. Our data show that the high–omega-3 diet, with an omega-6/omega-3 ratio recommended by nutritionists, could effectively deliver omega-3 PUFA to the prostate (Supplemental Figure 2), delay tumor formation (Figure 1) and progression (Figure 2), and prolong survival (Figure 5) as compared with the high–omega-6 diet. Mice on the low–omega-3 diet, with an omega-6/omega-3 ratio of 20 as compared with a ratio of 1 in the high–omega-3 diet, showed intermediary tumor growth, progression, and survival. Therefore, the omega-6/omega-3 ratio appears to be a critical factor in the effectiveness of prostate cancer suppression, with a higher proportion of omega-3 being more effective. However, the absolute amount of PUFAs may also be of consequence, since high total fat intake has been associated with cancer incidence (24). In the present study, all diets contained 13% fat with 30% energy from fat, mimicking the average Western diet, which is relatively high in fat. The development of normal prostate was not affected by the ratio of omega-6 to omega-3 in the *Pten* wild-type background. This demonstrates the importance of gene-diet interactions and that genetic cancer risk can be modified favorably by omega-3 PUFAs. It remains to be determined whether there is a critical omega-6/omega-3 ratio threshold for achieving maximal tumor suppression. Clinically, prostate cancer is usually diagnosed in men age 60 or older, and cancer cells proliferate slowly. Therefore, dietary and/or chemoprevention are of particular importance for the management of prostate cancer. Our data imply a beneficial effect of omega-3 PUFAs on delaying the onset of human prostate cancer. It will be interesting to determine whether any beneficial effects can also be achieved by supplementing the diet with omega-3 PUFAs after tumor initiation has occurred.

Table 1
PUFA ratios in *fat1* transgenic mice fed with high–omega-6 diet

Tissue	$Pten^{P-/-}fat1^{T/-}$			$Pten^{P-/-}fat1^{-/-}$		
	ω-3 (%)	ω-6 (%)	ω-6/ω-3 ratio	ω-3 (%)	ω-6 (%)	ω-6/ω-3 ratio
Blood	7.6	39.0	5.2	1.5	45.8	37.4
Prostate	3.8	16.8	4.4	0.54	24.8	45.9
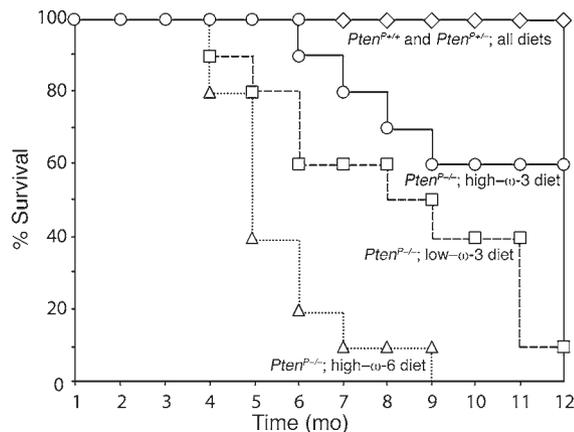
Lipid signaling plays a critical role in cancer of the prostate and many other human cancers. The *Pten* tumor suppressor gene is the most frequently mutated gene in metastases of prostate cancer (25, 26). A significant loss of *Pten* expression is also seen in prostate tumor tissues (27). Homozygous deletion of *Pten* in mouse prostate results in prostate cancer development and metastasis (28). In addition, the PI3K pathway appears to be a dominant growth factor–activated cell survival pathway in LNCaP prostate carcinoma cells (29). It was shown that PI3K/Akt stimulates the androgen pathway (30, 31), which further highlights the importance of lipid signaling in prostate cancer.

We showed that the high–omega-3 PUFA diet reduced phosphorylation of the downstream Akt target Bad and increased tumor cell death compared with the high–omega-6 PUFA diet in $Pten^{P-/-}$ mice (Figure 6). Knockdown of Bad in prostate cancer cells reduced the

percentage of dead cells upon omega-3 PUFA treatment to baseline levels (Figure 7B), and introduction of exogenous Bad restored the phenotype (Figure 7C). It is well documented that phospho-Bad protein is sequestered by 14-3-3 and that dephosphorylation allows Bad to interact with antiapoptotic proteins Bcl-2 and/or Bcl-xL, thereby increasing the Bax/Bcl-2 ratio and favoring apoptosis (32). Expression of a nonphosphorylatable form of Bad induces apoptosis in various cell lines, including prostate cancer cells (33–35). Why is the Bad protein differentially phosphorylated in tumors from mice on omega-3 and omega-6 diet? Preliminary data indicated that in $Pten^{P-/-}$ prostates from mice on the omega-6 diet, a large proportion of active Akt was localized to the plasma membrane, whereas on the omega-3 diet, active Akt tended to be distributed through the cytoplasm. The pattern of PI(3,4,5)P$_3$ localization coincided with that of the active Akt protein. The Akt kinase is activated by phosphoinositide binding (36, 37). In mammals, the *sn-1* position on the glycerol backbone of phospholipids, including phosphoinositides, is usually linked to a saturated FA such as stearic acid and the *sn-2* position often to an omega-6 PUFA such as arachidonic acid. Feeding cells or animals with omega-3 PUFAs results in replacement of omega-6 with omega-3 FAs at the *sn-2* position (38), which was verified in the blood and prostate tissue of our experimental mice (Supplemental Figure 2C).
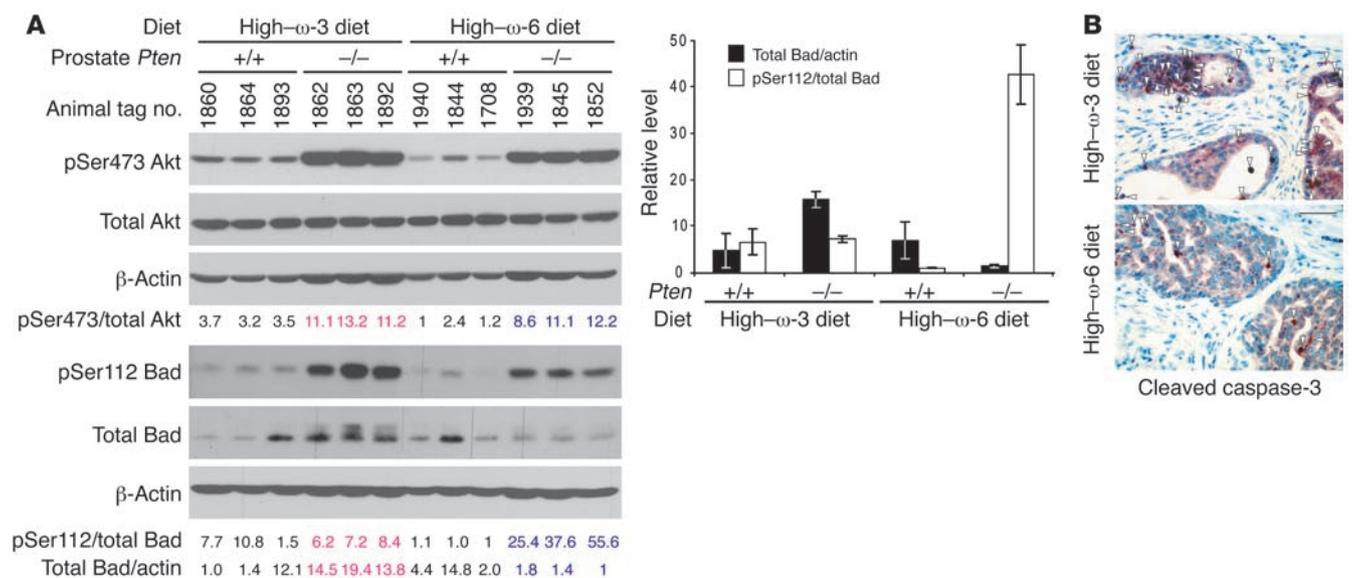

Figure 6
Alterations in Bad phosphorylation in vivo. (**A**) Protein extracts from the prostates of 8-week-old $Pten^{P+/+}$ and $Pten^{P-/-}$ mice fed the high–omega-3 and high–omega-6 diets were used for Western blotting analysis of Akt, pSer473 Akt, Bad, pSer112 Bad, and β-actin. Ratios of phospho-Akt to total Akt, phospho-Bad to total Bad, and total Bad to β-actin were calculated. Samples with the lowest ratio in each comparison were arbitrarily set as 1, and relative ratios are indicated at the bottom of the corresponding panels. Group averages and SEM for total Bad/β-actin and phospho-Bad/total Bad ratios are shown in the graph. (**B**) Immunohistochemistry for apoptotic cells was performed with an anti–cleaved caspase-3 antibody in prostate tissues of 8-week-old $Pten^{P-/-}$ mice. Arrowheads indicate apoptotic cells. Scale bar: 50 μm.

Table 2
Apoptotic index in tumor glands

Diet	Lobe		
	AP	**DL**	**VP**
High–ω-3	29.8	19.5	0[A]
High–ω-6	6.5	15.4	7.7

Apoptotic index was calculated as described in Methods. [A]All glands were either normal or hyperplastic, where no apoptosis was seen.

Therefore, it is possible that incorporation of omega-3 PUFAs into phospholipids could alter the localization of both PI(3,4,5)P$_3$ and the active form of Akt protein, resulting in differential Bad phosphorylation. On the other hand, it is also possible that this differential Bad phosphorylation is caused by a phosphatase. However, the nature of the enzymes involved in Bad dephosphorylation is somewhat controversial. Calcineurin and protein phosphatase 2A have been shown to dephosphorylate Bad in different cell types (39, 40). Experiments exploring the mechanism of Bad dephosphorylation in our system are ongoing.

We believe Bad-dependent modulation of apoptosis by omega-3 PUFAs to be a novel finding that could account, at least in part, for the proposed tumor-preventive properties of these FAs. In addition, omega-3 and -6 PUFAs can be metabolized by cyclooxygenases and lipoxygenases (41), and the resulting eicosanoids have different biological functions in processes such as proliferation, inflammation, and angiogenesis. These processes may contribute to carcinogenesis directly or indirectly. Indeed, we have noticed a reduction in microvessel density as well as CD3$^+$ lymphocyte levels in tumors from mice fed the omega-3 diet compared with those fed the high–omega-6 diet. The significance of these changes in relation to the suppression of prostate cancer by omega-3 PUFAs is currently under investigation.

Methods

Mice

Prostate-specific *Pten*-knockout mice were generated by crossing *Pten$^{loxP/loxP}$* mice (42) with mice of the ARR2Probasin-*cre* transgenic line *PB-cre4*, wherein the Cre recombinase is under the control of a modified rat prostate-specific probasin promoter (43), as previously reported (44). B6.129S4-Gt(ROSA)26Sor^{tm1Sor}/J mice, which have a floxed *lacZ* gene targeted to the *ROSA26* locus, whose expression depends on Cre activity, were purchased from The Jackson Laboratory. For simplicity, *Pten$^{loxP/loxP}$PB-cre4$^{-/-}$* and *Pten$^{loxP/+}$PB-cre4$^{-/-}$* are referred to as *Pten$^{P+/+}$*; *Pten$^{loxP/+}$PB-cre4$^{T/-}$* as *Pten$^{P+/-}$*; *Pten$^{loxP/loxP}$PB-cre4$^{T/-}$* as *Pten$^{P-/-}$*; and *B6.129S4-Gt(ROSA)26Sor^{tm1Sor}/J* as *ROSA26$^{LZ/LZ}$*. F$_1$ and F$_2$ mice were maintained on experimental diets, and only F$_2$ males were used in our experiments.

fat1-transgenic mice (14) were crossed with prostate-specific *Pten*-knockout mice. *Pten$^{P-/-}$fat1$^{T/-}$* and *Pten$^{P-/-}$fat1$^{-/-}$* mice were used in this study.

The *PB-cre4*, *ROSA26$^{LZ/LZ}$*, and *fat1* transgenic mice were of a congenic C57BL/6 background. They were backcrossed to C57BL/6 for more than 10 generations. The *Pten$^{loxP/loxP}$* mice were of mixed C57BL/6 and BALB/c background. They were backcrossed to C57BL/6 for 3–5 generations.

Histopathological evaluation of mouse prostate tissues was performed by board-certified veterinary pathologists. The Bar Harbor classification system for scoring the benign and malignant growth in the prostates of genetically engineered mice was used (45). However, the authors prefer the term "carcinoma in situ" to "mPIN" (mouse prostatic intraepithelial neoplasia), as it

accurately describes a preinvasive carcinoma lesion without requiring further clarification. Human PIN lesions, while being predictive of the development of an invasive adenocarcinoma, do not demonstrate direct invasion through the basement membrane into the surrounding stroma as the neoplastic epithelial lesions were seen to do in these transgenic mouse prostate glands.

All animals were maintained in an isolated environment in barrier cages and fed the specified diet. Animal care was conducted in compliance with the state and federal Animal Welfare Acts and the standards and policies of the US Department of Health and Human Services. The protocol was approved by our Institutional Animal Care and Use Committee at Wake Forest University.

Diet

Diets were prepared by the custom animal diet laboratory of the Animal Resources Program at Wake Forest University. All 3 diets contained 397 kcal/100 g, and 30% of energy was from fat, 50% from carbohydrates, and 30% from proteins. The omega-6/omega-3 ratio was 1 in the high–omega-3 diet, 20 in the low–omega-3 diet, and 40 in the high–omega-6 diet (Figure 1B and Supplemental Table 1).

Blood collection

Prior to sacrifice of animals, approximately 200 μl of blood per mouse was collected through the retro-orbital vein, snap-frozen in liquid nitrogen, and stored at –80°C until analysis.

FA and phospholipid analysis

Lipid extractions and FA analysis. Total FAs were analyzed in the food, blood, and prostate of mice at the ages of 5, 8, and 12 weeks (5 mice per group). Internal standards, 1,2-dipentadecanoylglycero-3-phosphocholine and 1,2-didodecanoylglyceero-3-phosphoethanolamine, were added to each tube, and solvent was removed in a stream of Ar. The residue was dissolved in 1 ml of ethanol and then mixed with 10 μl of sample. Tissue was extracted using the method of Bligh and Dyer (46), with di-15:0 phosphatidylcholine (PC) or di-12:0 phosphatidylethanolamine (PE) as an internal standard. After extraction, the supernatant was decanted and saved. Protein pellets were saved for later analysis. Organic layers were combined and evaporated under a stream of Ar at 37°C then redissolved in 1 ml of ethanol. Sample preparation was based on the method of Metcalfe et al. (47) as used previously (48). The sample in ethanol was treated with 0.1 ml of 50% aqueous KOH, the tube was purged with Ar, and then heated to 60°C for 1 hour. After cooling, nonsaponifiable lipids were removed by extracting with 3 ml of hexane. The aqueous layer was acidified and extracted with 3 ml of hexane, and the hexane layer was removed and dried in a stream of Ar. The residue was treated with 0.5 M methanolic NaOH at 100°C for 5 minutes. After cooling, the sample was treated with 1 ml of 14% BF$_3$ in methanol (Sigma-Aldrich), flushed with Ar, and then heated to 100°C for 5 minutes. After cooling, the samples were treated with 2 ml of hexane and 4 ml of saturated, aqueous NaCl. The hexane phase was transferred to a separate tube, dried in a stream of Ar, then diluted with hexane (500 μl for blood samples or 50 μl for tissue samples), and then 1 μl of solution was analyzed on a Trace MS interfaced to a Trace 2000 GC (Thermo Electron Corp.). Separation was accomplished using a 30 m × 0.25 mm diameter DB-WAX WCOT column (Agilent Technologies) with a 0.25-μm coating.

Phospholipid analysis. Tissue was extracted as described above and dissolved in 1 ml of CHCl$_3$/MeOH (1:1, vol/vol). Blood was extracted by adding 10 μl of blood to 5 ml hexane/isopropanol (3:2, vol/vol) containing the internal standard d-15:0 PC or di-12:0 PE. After flushing the headspace with Ar and extracting for 1 hour at room temperature, the sample was centrifuged and supernatant decanted. Solvent was removed in a stream of Ar and sample redissolved in 1 ml of CHCl$_3$/MeOH (1:1, vol/vol). Total phosphorus was
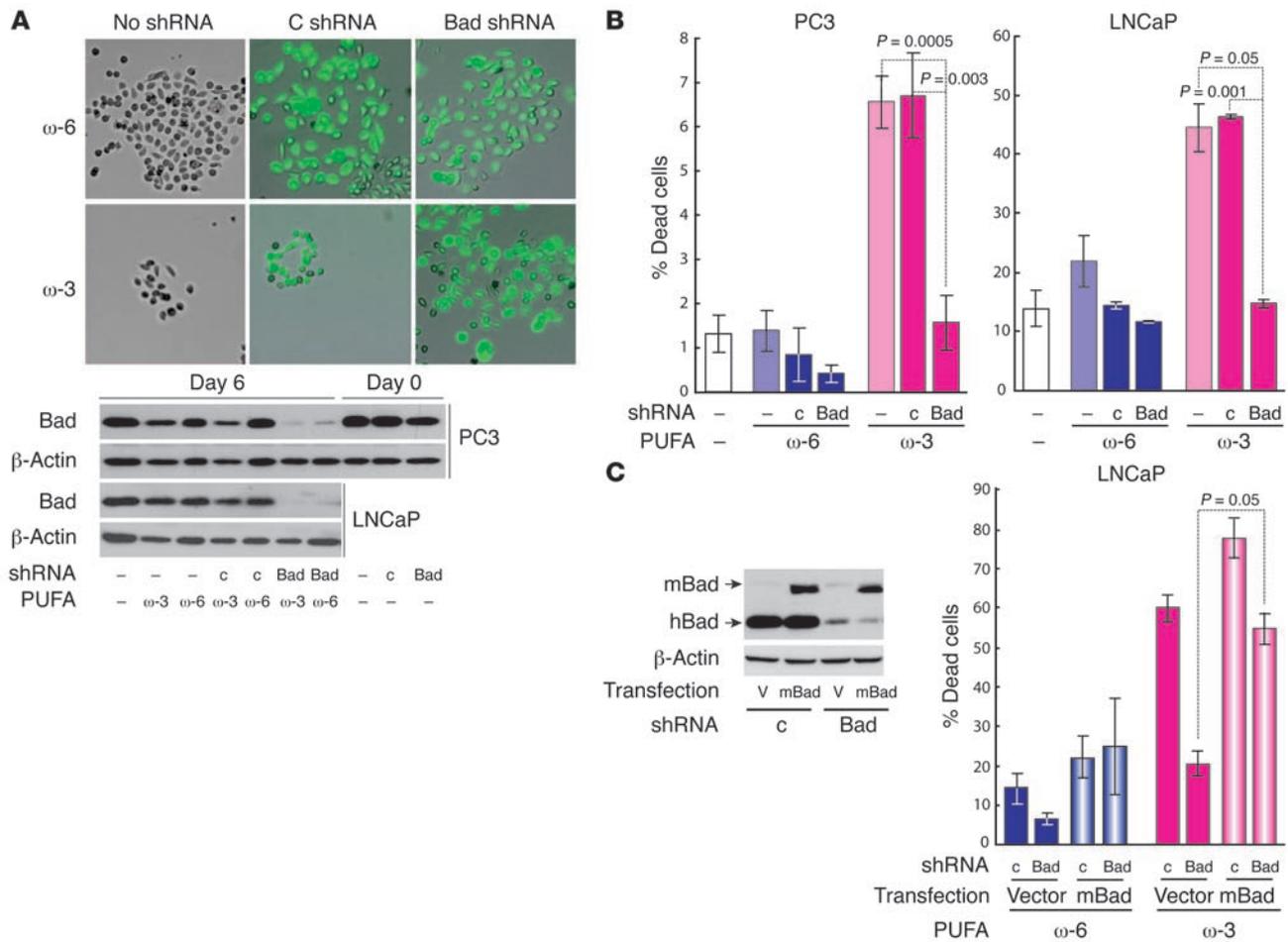
Figure 7
Dependence on Bad for omega-3 PUFA–induced cell death. (**A**) PC3 cells were infected with lentivirus expressing scrambled shRNA (C shRNA) or Bad-specific shRNA (Bad shRNA) or mock infected (no shRNA) for 2 days. Cells were seeded and incubated with FAs for 6 days, then photographed using a fluorescence microscope. The presence of lentivirus is evidenced by GFP expression. Western blotting was performed to confirm the successful knockdown of Bad in both PC3 and LNCaP cells. Day 0, prior to FA treatment; day 6, after incubation with media containing FA for 6 days. C, control. (**B**) Live and dead cells were enumerated by the trypan blue exclusion method using a hemocytometer. *P* values were determined by Student's *t* test. LNCaP cells have higher background apoptosis compared with PC3 cells, but omega-3 FA treatment increased apoptosis approximately 4-fold in both cell lines.(**C**) LNCaP cells were transfected with control vector or mouse Bad expression vector. G418-resistant colonies were isolated, verified for successful expression of the HA-tagged mouse Bad by Western blotting, and pooled. Vector control– (V) and mouse Bad–expressing (mBad) LNCaP cells were infected with shRNA lentivirus as described above. Cells were incubated with FAs for 6 days, and live and dead cells were enumerated as described above. Cell lysates were used for confirmation of successful knockdown of the endogenous Bad but not the exogenous mouse Bad (whose sequence varies from human Bad in the region targeted by the shRNA).

analyzed using the method of Rouser et al. (49). Samples were diluted to 2 nmol/ml in CHCl$_3$/MeOH (1:1, vol/vol) containing 1% formic acid for analysis and analyzed using a Quattro II electrospray triple quadrupole tandem mass spectrometer (Waters Corp.) as previously described (50). Precursor-ion analysis at 184 *m/z* in the positive ion mode identified PC molecular species. PE and phosphatidylserine (PS) molecular species were identified in the positive-ion mode by monitoring the common-neutral losses of 141 Da and 185 Da, respectively. The FA distribution of individual molecular species was determined in the negative-ion mode by product ion analysis of [M-CH$_3$]-ions from PC, PE, or PS. The ion intensity of each spectrum was corrected for isotope effects and transmission losses.

Prostate tissue dissection and processing
The AP, DL, and VP lobes were dissected as described previously (44). Whole mouse and prostate were weighed. Prostate tissues were paraffin embedded

for histology and immunohistochemistry, pulverized in liquid nitrogen for lipid analysis, homogenized in a buffer for Western blotting, or snap-frozen and OCT embedded for immunostaining of phosphoinositides.

Survival experiments
A cohort of 90 mice (10 mice per group for *Pten*$^{P+/+}$, *Pten*$^{P+/–}$, and *Pten*$^{P–/–}$ mice on each of the 3 experimental diets) was followed for 12 months. Time to death was recorded. Death was either natural or by euthanasia (if mice were moribund), as recommended by veterinarians according to institutional policies.

Immunohistochemistry
Cleaved caspase-3 staining was performed with an anti–cleaved caspase-3 primary antibody (catalog 9661; Cell Signaling Technology), followed by a biotinylated anti-rabbit secondary antibody and streptavidin alkaline

phosphatase (Super Sensitive Link-Label IHC Detection Systems; Bio-Genex), visualized with Vector Red Substrate (SK-5100; Vector Laboratories), and counterstained with hematoxylin. Representative whole prostate sections for omega-3– and omega-6–fed $Pten^{P-/-}$ mice were photographed in their entirety, and each VP, DL, and AP lobe was assembled by tiling individual images in Adobe Photoshop CS (Adobe Systems Inc.). The total number of epithelial cells was enumerated in all glands using Image-Pro Plus 4.5 software (Image Processing Solutions). Numbers of apoptotic cells were counted in every gland under a light microscope by 2 individuals. The apoptotic index for each prostate lobe was expressed as the number of apoptotic cells per thousand cells in tumor glands (glands with normal and hyperplastic morphology were excluded). Average apoptotic indices are presented.

Western blotting

Prostate tissues were homogenized or cells were lysed in a buffer (50 mM Tris-HCl pH 7.5, 150 mM NaCl, 0.5% NP-40, 1 mM DTT, 1 mM PMSF, 1× Protease Inhibitors [catalog 1697498; Roche Applied Science]) with phosphatase inhibitors (50 mM NaF, 1 mM Na$_3$VO$_4$, 50 mM β-glycerophosphate, and 40 mM p-nitrophenylphosphate). Western blotting was performed as described previously (51) with anti–pS437 Akt (catalog 3787), anti–total Akt (catalog 9272), anti–Bad pSer112 (catalog 9291), anti–total Bad (catalog 9292), anti–phosphorylated FoxO1 and -3a (catalog 9464), and anti–S6K pT389 (catalog 9205) antibodies (Cell Signaling Technology), as well as anti–β-actin (Sigma-Aldrich).

Assessment of Pten deletion rate

Real-time PCR quantitation of Pten Δ5 allele. Prostate genomic DNA was extracted from 6-, 7-, and, 8-week-old $Pten^{P-/-}$ mice and diluted to final concentration of 100 ng/μl. Real-time PCR was performed for $Pten$ lacking exon 5 and Il-2 (as a single copy number control) alleles using iCycler (Bio-Rad) with QuantiTect SYBR Green PCR kit (QIAGEN), using 100 ng genomic DNA per reaction. PCR reaction consisted of 50 cycles of 15 seconds at 94°C, 30 seconds at 57°C, and 45 seconds at 72°C. Reaction mixtures without genomic DNA were used as negative controls. Primers used were 5′-TCCCAGAGTTCATACCAGGA-3′ and 5′-GCAATGGCCAGTAC-TAGTGAAC-3′ for $Pten$ Δ5; and 5′-CTAGGCCACAGAATTGAAAGATCT-3′ and 5′-GTAGGTGGAAATTCTAGCATCATCC-3′ for Il-2. For each primer set, a standard curve was constructed with dilutions of a reference genomic DNA sample. Three mice were used per data point, and each sample was analyzed in triplicate. Amounts of $Pten$ Δ5 were normalized to Il-2, and average values were presented.

LacZ activity assay. $Pten^{loxP/loxP}ROSA26^{LZ/LZ}PB$-$cre4^{T/-}$ mice were generated by crossing $Pten^{L/+}ROSA26^{LZ/+}PB$-$cre4^{T/-}$ males with $Pten^{loxP/loxP}ROSA26^{LZ/LZ}$ females. In these mice, the Cre recombinase is expressed in prostate epithelial cells under the control of the probasin promoter, and an inactive allele of the $lacZ$ gene under ubiquitously active $ROSA26$ promoter. Cre-mediated recombination at $loxP$ sites in the $lacZ$ gene activated expression of catalytically active β-galactosidase (Figure 3A), whereas recombination at $loxP$ sites in the $Pten$ gene inactivated $Pten$. Prostate tissues from 6-week-old $Pten^{loxP/loxP}ROSA26^{LZ/LZ}PB$-$cre4^{T/-}$ mice were homogenized in Promega passive lysis buffer with 0.2 mM PMSF and 1 mM DTT. After 3 freeze-thaw cycles, tissue debris was removed by centrifugation at 16,000 g for 15 minutes. Protein concentration was measured with a Pierce BCA kit, and equal amounts of protein were assayed for β-galactosidase activity using Beta-Glo assay system (Promega). Briefly, 35 μl diluted sample was incubated with 35 μl Beta-Glo reagent for 45 minutes at room temperature. RLU were read on a TD-20120 luminometer (Turner Designs Inc.). Protein lysates from $Pten^{loxP/loxP}ROSA26^{LZ/LZ}PB$-$cre4^{-/-}$ mice were used as negative controls for background subtraction. Three mice per data point were used, and each sample was analyzed in duplicate. Averaged values with SEM are presented.

β-Galactosidase staining. Portions of prostate tissues from the mice described above were snap frozen and OCT embedded. Sections (8-μm) were cut, fixed (2% formaldehyde, 0.2% glutaraldehyde in PBS) for 5 minutes. After 3 washes in PBS, sections were incubated in X-Gal staining solution (1 mg/ml X-Gal, 4 mM potassium ferricyanide, 4 mM potassium ferrocyanide, 2 mM magnesium chloride, 0.02% IGEPAL CA-630, 0.01% sodium deoxycholate) at 37°C for 2.5 hours. Finally, sections were washed in distilled water, counterstained with eosin, dehydrated, and mounted.

Akt Western blotting. Protein lysates obtained as described above for the β-galactosidase activity assay were also used for Western blotting of pSer473 and total Akt as described in "Western blotting."

Bad knockdown

To generate shRNA virus, Bad targeting sequence 5′-GGCTTG-GTCCCATCGGAAG*ttcaagaga*CTTCCGATGGGACCAAGCC-3′ (human Bad sequence in capital letters and loop in italics) was cloned between the XhoI and HpaI sites into the pLL3.7 lentiviral vector, which has a GFP marker. A scrambled sequence 5′-GGTACGGTCAG-GCAGCTTCT*ttcaagaga*AGAAGCTGCCTGACCGTACC-3′ was used as control. HEK293 cells were transfected with shRNA vector together with packaging vectors (VSVG, RSV-REV, and pMDLg/pRRE). Supernatants were collected 48 hours after transfection.

PC3, LNCaP, or LNCaP transfected with control vector and mouse Bad expression vector were used in knockdown experiments. Due to sequence variations, mouse cDNA is not susceptible to knockdown with our shRNA designed to target human Bad. G418-resistant colonies were isolated, verified for successful expression of the HA-tagged mouse Bad by Western blotting, and pooled. PC3, LNCaP, LNCaP (vector), and LNCaP (mBad) cells were infected with shRNA lentivirus expressing scrambled shRNA or Bad-specific shRNA or were mock infected for 2 days. Cells (10,000) were seeded in 6-well plates with 1 ml medium with or without 100 μg/ml LDL FAs (15). One milliliter of corresponding fresh medium was added every other day, and cells were incubated for a total of 6 days. Cells were enumerated by the trypan blue exclusion method. Cells were collected after counting and used for Western blotting of Bad and β-actin.

Statistics

Mouse prostate weight data were analyzed using a 2-way ANOVA model. In these models, prostate weight adjusted for body weight (mg/25 g) was considered the outcome. The 2 factors of interest were treatment (mice were randomly assigned to each of the 3 groups: high–omega-3, low–omega-3, and high–omega-6) and age of mouse (4 levels: 5, 8, 12, and 24 weeks). In addition, the treatment-by-age interaction was examined in these models. The data was examined for assumptions of ANOVA modeling (homogeneity of variances, normality, etc.), and there did not appear to be any severe deviations. Significance testing was performed using 2-sided tests with α = 0.05 for all comparisons. For all ANOVA analyses, data for all mice were used (i.e., no mice needed to be excluded). Survival data were compared between treatment groups using Cox proportional hazards regression models. In these comparisons, 6 groups of mice had no events (all $Pten^{P+/+}$ and $Pten^{P+/-}$ mice survived), so the inference was made based on the 3 $Pten^{P-/-}$ groups. Hazard ratios and P values were calculated using a 2-sided 0.05 α value to determine statistical significance. Pairwise comparisons were made between the high–omega-6 diet and the other 2 diets separately.

1. Kolonel, L.N. 2001. Fat, meat, and prostate cancer. *Epidemiol. Rev.* **23**:72–81.
2. Wynder, E.L., Mabuchi, K., and Whitmore, W.F., Jr. 1971. Epidemiology of cancer of the prostate. *Cancer.* **28**:344–360.
3. Breslow, N., et al. 1977. Latent carcinoma of prostate at autopsy in seven areas. The International Agency for Research on Cancer. Lyon, France. *Int. J. Cancer.* **20**:680–688.
4. Dunn, J.E. 1975. Cancer epidemiology in populations of the United States — with emphasis on Hawaii and California — and Japan. *Cancer Res.* **35**:3240–3245.
5. Haenszel, W., and Kurihara, M. 1968. Studies of Japanese migrants. I. Mortality from cancer and other diseases among Japanese in the United States. *J. Natl. Cancer Inst.* **40**:43–68.
6. Staszewski, J., and Haenszel, W. 1965. Cancer mortality among the Polish-born in the United States. *J. Natl. Cancer Inst.* **35**:291–297.
7. Simopoulos, A.P., Leaf, A., and Salem, N., Jr. 1999. Essentiality of and recommended dietary intakes for omega-6 and omega-3 fatty acids. *Ann. Nutr. Metab.* **43**:127–130.
8. Dewailly, E., et al. 2001. n-3 fatty acids and cardiovascular disease risk factors among the Inuit of Nunavik. *Am. J. Clin. Nutr.* **74**:464–473.
9. Simopoulos, A.P. 1999. Essential fatty acids in health and chronic disease. *Am. J. Clin. Nutr.* **70**(3 Suppl.):560S–569S.
10. Weber, P.C. 1989. Are we what we eat? Fatty acids in nutrition and in cell membranes: cell functions and disorders induced by dietary conditions. In *Fish, fats and your health. Proceedings of the International Conference on Fish Lipids and Their Influence on Human Health.* August 9–11. Svanoy, Norway. Svanoy Foundation. 9–18.
11. Giardiello, F.M., et al. 1993. Treatment of colonic and rectal adenomas with sulindac in familial adenomatous polyposis. *N. Engl. J. Med.* **328**:1313–1316.
12. Jacobs, E.J., et al. 2005. A large cohort study of aspirin and other nonsteroidal anti-inflammatory drugs and prostate cancer incidence. *J. Natl. Cancer Inst.* **97**:975–980.
13. Solomon, S.D., et al. 2005. Cardiovascular risk associated with celecoxib in a clinical trial for colorectal adenoma prevention. *N. Engl. J. Med.* **352**:1071–1080.
14. Kang, J.X., Wang, J., Wu, L., and Kang, Z.B. 2004. Transgenic mice: fat-1 mice convert n–6 to n–3 fatty acids. *Nature.* **427**:504.
15. Edwards, I.J., et al. 2004. Differential effects of delivery of omega-3 fatty acids to human cancer cells by low-density lipoproteins versus albumin. *Clin. Cancer Res.* **10**:8275–8283.
16. Feinberg, A.P., and Tycko, B. 2004. The history of cancer epigenetics. *Nat. Rev. Cancer.* **4**:143–153.
17. Feinberg, A.P. 2004. The epigenetics of cancer etiology. *Semin. Cancer Biol.* **14**:427–432.
18. Lund, A.H., and van Lohuizen, M. 2004. Epigenetics and cancer. *Genes Dev.* **18**:2315–2335.
19. Norrish, A.E., Skeaff, C.M., Arribas, G.L., Sharpe, S.J., and Jackson, R.T. 1999. Prostate cancer risk and consumption of fish oils: a dietary biomarker-based case-control study. *Br. J. Cancer.* **81**:1238–1242.
20. Terry, P., Lichtenstein, P., Feychting, M., Ahlbom, A., and Wolk, A. 2001. Fatty fish consumption and risk of prostate cancer. *Lancet.* **357**:1764–1766.
21. Yang, Y.J., Lee, S.H., Hong, S.J., and Chung, B.C. 1999. Comparison of fatty acid profiles in the serum of patients with prostate cancer and benign prostatic hyperplasia. *Clin. Biochem.* **32**:405–409.
22. Freeman, V.L., et al. 2000. Prostatic levels of fatty acids and the histopathology of localized prostate cancer. *J. Urol.* **164**:2168–2172.
23. Augustsson, K., et al. 2003. A prospective study of intake of fish and marine fatty acids and prostate cancer. *Cancer Epidemiol. Biomarkers Prev.* **12**:64–67.
24. Hursting, S.D., Thornquist, M., and Henderson, M.M. 1990. Types of dietary fat and the incidence of cancer at five sites. *Prev. Med.* **19**:242–253.
25. Suzuki, H., et al. 1998. Interfocal heterogeneity of PTEN/MMAC1 gene alterations in multiple metastatic prostate cancer tissues. *Cancer Res.* **58**:204–209.
26. Vlietstra, R.J., van Alewijk, D.C., Hermans, K.G., van Steenbrugge, G.J., and Trapman, J. 1998. Frequent inactivation of PTEN in prostate cancer cell lines and xenografts. *Cancer Res.* **58**:2720–2723.
27. McMenamin, M.E., et al. 1999. Loss of PTEN expression in paraffin-embedded primary prostate cancer correlates with high Gleason score and advanced stage. *Cancer Res.* **59**:4291–4296.
28. Wang, S., et al. 2003. Prostate-specific deletion of the murine Pten tumor suppressor gene leads to metastatic prostate cancer. *Cancer Cell.* **4**:209–221.
29. Lin, J., Adam, R.M., Santiestevan, E., and Freeman, M.R. 1999. The phosphatidylinositol 3′-kinase pathway is a dominant growth factor-activated cell survival pathway in LNCaP human prostate carcinoma cells. *Cancer Res.* **59**:2891–2897.
30. Sharma, M., Chuang, W.W., and Sun, Z. 2002. Phosphatidylinositol 3-kinase/Akt stimulates androgen pathway through GSK3beta inhibition and nuclear beta-catenin accumulation. *J. Biol. Chem.* **277**:30935–30941.
31. Manin, M., et al. 2002. Androgen receptor expression is regulated by the phosphoinositide 3-kinase/Akt pathway in normal and tumoral epithelial cells. *Biochem. J.* **366**:729–736.
32. Danial, N.N., and Korsmeyer, S.J. 2004. Cell death: critical control points. *Cell.* **116**:205–219.
33. Datta, S.R., et al. 2000. 14-3-3 proteins and survival kinases cooperate to inactivate BAD by BH3 domain phosphorylation. *Mol. Cell.* **6**:41–51.
34. Sastry, K.S., Smith, A.J., Karpova, Y., Datta, S.R., and Kulik, G. 2006. Diverse antiapoptotic signaling pathways activated by vasoactive intestinal polypeptide, epidermal growth factor, and phosphatidylinositol 3-kinase in prostate cancer cells converge on BAD. *J. Biol. Chem.* **281**:20891–20901.
35. She, Q.B., et al. 2005. The BAD protein integrates survival signaling by EGFR/MAPK and PI3K/Akt kinase pathways in PTEN-deficient tumor cells. *Cancer Cell.* **8**:287–297.
36. Klippel, A., Kavanaugh, W.M., Pot, D., and Williams, L.T. 1997. A specific product of phosphatidylinositol 3-kinase directly activates the protein kinase Akt through its pleckstrin homology domain. *Mol. Cell. Biol.* **17**:338–344.
37. Stocker, H., et al. 2002. Living with lethal PIP3 levels: viability of flies lacking PTEN restored by a PH domain mutation in Akt/PKB. *Science.* **295**:2088–2091.
38. Chabot, M.C., Schmitt, J.D., Bullock, B.C., and Wykle, R.L. 1987. Reacylation of platelet activating factor with eicosapentaenoic acid in fish-oil-enriched monkey neutrophils. *Biochim. Biophys. Acta.* **922**:214–220.
39. Wang, H.G., et al. 1999. Ca2+-induced apoptosis through calcineurin dephosphorylation of BAD. *Science.* **284**:339–343.
40. Chiang, C.W., et al. 2003. Protein phosphatase 2A dephosphorylation of phosphoserine 112 plays the gatekeeper role for BAD-mediated apoptosis. *Mol. Cell. Biol.* **23**:6350–6362.
41. Larsson, S.C., Kumlin, M., Ingelman-Sundberg, M., and Wolk, A. 2004. Dietary long-chain n-3 fatty acids for the prevention of cancer: a review of potential mechanisms. *Am. J. Clin. Nutr.* **79**:935–945.
42. Lesche, R., et al. 2002. Cre/loxP-mediated inactivation of the murine Pten tumor suppressor gene. *Genesis.* **32**:148–149.
43. Wu, X., et al. 2001. Generation of a prostate epithelial cell-specific Cre transgenic mouse model for tissue-specific gene ablation. *Mech. Dev.* **101**:61–69.
44. Berquin, I.M., Min, Y., Wu, R., Wu, H., and Chen, Y.Q. 2005. Expression signature of the mouse prostate. *J. Biol. Chem.* **280**:36442–36451.
45. Shappell, S.B., et al. 2004. Prostate pathology of genetically engineered mice: definitions and classification. The consensus report from the Bar Harbor meeting of the Mouse Models of Human Cancer Consortium Prostate Pathology Committee. *Cancer Res.* **64**:2270–2305.
46. Bligh, E.G., and Dyer, W.J. 1959. A rapid method of total lipid extraction and purification. *Can. J. Biochem. Physiol.* **37**:911–917.
47. Metcalfe, L.D., Schmitz, A.A., and Pelka, J.R. 1966. Rapid preparation of fatty acid esters from lipids for gas chromatographic analysis. *Anal. Chem.* **38**:514–515.
48. Schwenke, D.C., Rudel, L.L., Sorci-Thomas, M.G., and Thomas, M.J. 2002. Alpha-tocopherol protects against diet induced atherosclerosis in New Zealand white rabbits. *J. Lipid Res.* **43**:1927–1938.
49. Rouser, G., Siakotas, A.N., and Fleisher, S. 1966. Quantitative analysis of phospholipids by thin-layer chromatography and phosphorus analysis of spots. *Lipids.* **1**:85–86.
50. DeLong, C.J., Baker, P.R., Samuel, M., Cui, Z., and Thomas, M.J. 2001. Molecular species composition of rat liver phospholipids by ESI-MS/MS: the effect of chromatography. *J. Lipid Res.* **42**:1959–1968.
51. Liu, J., et al. 2002. Mediation of the DCC apoptotic signal by DIP13 alpha. *J. Biol. Chem.* **277**:26281–26285.